Manufacturing of anti-fogging Super-hydrophilic Microstructures on Glass by Nanosecond Laser

Liang Yang[1 iD], Xichun Luo[2*], Wenlong Chang[2], Yankang Tian[2], Zhengjian Wang[2], Jian Gao[2], Yukui Cai[3], Yi Qin[2], Mark Duxbury[4]

1. School of Mechanical Engineering, Dalian Jiaotong University, P.R.China. 3000yangliang@163.com
2. Centre for Precision Manufacturing, DMEM, University of Strathclyde, Glasgow G1 1XJ, UK Wenlong.chang@strath.ac.uk, Yankang.Tian@strath.ac.uk, Zhengjian.wang@strath.ac.uk, Jian.Gao@strath.ac.uk, Yi.qin@strath.ac.uk
3. School of Mechanical Engineering, Shandong University, P.R. China, caiyukui@mail.sdu.edu.cn
4. Department of Surgery, Glasgow Royal Infirmary, UK, mduxbury@nhs.net

* Correspondence: xichun.luo@strath.ac.uk; Tel.: +44-(0)-141-574-5280

Abstract:

In this paper, a nanosecond laser processing method with the support of light-absorption auxiliary materials was developed to fabricate anti-fogging super-hydrophilic microstructures on glass substrate surfaces. Through adjusting the focal point offset, the laser was focused on the auxiliary material layer, thus the laser energy required for micromachining was precisely controlled. As a processing example, a bionic honeycomb structure was successfully manufactured by this method. The effects of laser processing parameters on the size and integrity of the fabricated microstructures and on the light transmission of the machined surface were investigated through laser machining experiment. The results indicate that lower power and frequency is the key to obtaining regular honeycomb structures in laser machining. The laser focal point significantly affects the light transmittance of glass, while the feed rate has little effect. The water droplet contact angle was measured to evaluate the hydrophilicity of glass specimens with different dimensions of microstructure. It was found that the contact angle decreased with reduction of the honeycomb structure size.

Keywords: Hydrophilicity surface, Glass, Nanosecond laser machining, Honeycomb structure

1. Introduction

Transparent materials such as glass and some polymers are widely used as mirrors and windows, finding applications in protective equipment such as goggles, solar cell protection layers, scientific microscopes, cameras and medical devices such as endoscopes. However, under certain conditions,

such as low temperature or high humidity, fogging occurs on the surface of these transparent materials; adversely affect its optical qualities and impairing function. Fogging on the lens of medical endoscope during surgery can prevent the operation from proceeding normally and may even result in a medical error and endanger life [1][2]. The research and development of anti-fogging technologies and materials have therefore attracted extensive attention in the scientific and medical device communities.

Fogging is a process in which water vapour condenses into small droplets on a surface. Each small water droplet will refract and reflect light, thereby significantly reducing the light transmittance of the normally transparent substrate and affecting its optical qualities. The conditions required for fogging to occur can be divided into two aspects: (1) the existence of certain humidity and temperature differences in the external environment. (2) whether the wetting property of the substrate surface is atomized or not depends on the surface tension among the three phases of gas, liquid and solid: when the surface energy of a solid is large enough, small liquid droplets spread and cause less fogging[3]. Conversely, liquids on a solid with low surface energy will tend to form discrete droplets, resulting in fogging.

Some anti-fogging measures were therefore proposed to modify these conditions. Currently, changing wettability of the substrate surface, i.e. through preparation of hydrophilic or even super-hydrophilic surfaces to improve the affinity between the solid surface and the water drops, is an important anti-fogging strategy. There are two ways to achieve hydrophilic or super hydrophilicity on the surfaces, i.e. by application of a coating or through surface modification with micro/nano structuring [4]. For example, Nanocomposite coatings [5], vapour deposition [6], Liquid-Phase Deposition (LPD)[7], spin coating[8] etc. have been used to coat. Etching [9], layer-by-layer assembly [10], sol-gel chemistry [11], hydrothermal treatment[12], successive ionic layer adsorption and reaction (SILAR)[13], hydrothermal synthesis[14], electrochemical micromachining (EMM)[15], abrasive water jet micro-machining[16][17] have been used to generate microstructures. However, fabrication of hydrophilic microstructures on glass while maintaining the

transparency of the microstructured glass remains challenging. A systematic approach for design of hydrophilic or superhydrophilic micro/nano structures on transparent material surfaces without impairing light transmission and a cost-effective manufacturing approach for generation of such micro/nano structures with low environmental impact are the target results of ongoing research. This paper concerns the development of a nanosecond laser machining process for the generation of anti-fogging super-hydrophilic microstructures on glass without affecting its light transmission capability. Following a review of current nanosecond laser machining techniques the concept of bio-inspired microstructures will be introduced. The experimental design and setup will be detailed in section 4, while the results and discussions will be presented in section 5 followed by our conclusions.

2. Literature review on nanosecond laser microstructuring research

Nanosecond laser machining is a good candidate for cost-effective manufacturing of microstructures due to its high efficiency and contactless characteristics. The technique has been used for the manufacture of microstructures, such as micro-holes, micro channels and micropatterns on different materials by various researchers. For example, nanosecond laser machining has been used to drill micro-holes sapphire with black paint as the solid backing layer [18]. Micro-cavity structures have also been generated by using a high fluence nanosecond pulsed fiber laser, assisted with high pressure co-axial Argon gas on silicon carbide (SiCp)/AA2024 matrix composites [19]. Microchannels can be generated on silicon compound ceramics in water [20] and on polymethylmethacrylate (PMMA) [21]. The technique can create multi-depth microchannel networks on silicon, which can then be subjected to chemical etching [22]. Nanosecond laser has also been successfully applied to successfully fabricate hydrophilic microstructures on variety of materials, such as stainless steel[23]-[26], titanium[27], polycrystalline Si[28], Ag/Co[29], ABS copolymer[30], polyethylene[31], aluminium[32]-[34][35], nickel[36], copper and brass[37], Mg alloy[38], Inconel 718[39] to change their wettability.

Surface microstructuring processes have stringent requirements on dimensions, especially on the depth of microstructures. Although nanosecond laser has been used by researchers [40][41] to drill holes because of the small radial size and depth of the designed microstructures, nanosecond laser microstructuring process on glass is still rarely performed and remains technically challenging. The technique is affected by specific technical problems: First, the precise control of a nanosecond laser is very difficult, especially at red wavelengths, because this kind of short pulse laser has very large beam energy density, which results in a large thermal damage zone on the generated microstructures. In addition, a large energy density will degrade the form accuracy and the surface integrity of the fabricated microstructures, further affecting its design functionality and light transmission. Second, the glass material itself has good light transmittance, and has extremely low absorption capacity for nanosecond lasers wavelengths. Therefore, it is difficult for the laser to focus on the glass surface and complete the ablation process during processing.

This paper will describe a nanosecond laser processing method with the support of absorption-aiding materials to overcome these challenges and propose a deterministic manufacturing approach to obtain micro/nano structures on glass by use of nanosecond laser.

3. A bio-inspired micro structure

Inspiration for the design of functional structures often comes from nature. Through the study of natural biological structures, bio-inspired surface structures for the antireflective, self-cleaning and drag reducing surfaces, as well as new types of adhesive systems have been created [42]. Liu et al[43] studied antifogging mosquito eyes and designed an artificial compound eye structure based on hexagonal structure, which has special wetting properties. We present a new micro-porous hexagonal structure, termed the honeycomb structure, which is based on a Gaussian groove processed by laser.

The design of honeycomb hole arrays is shown in Fig.1. Where *P* is the pitch between two adjacent hexagonal holes, *L* is the length of the hexagonal structure and *b* represents the wall thickness.

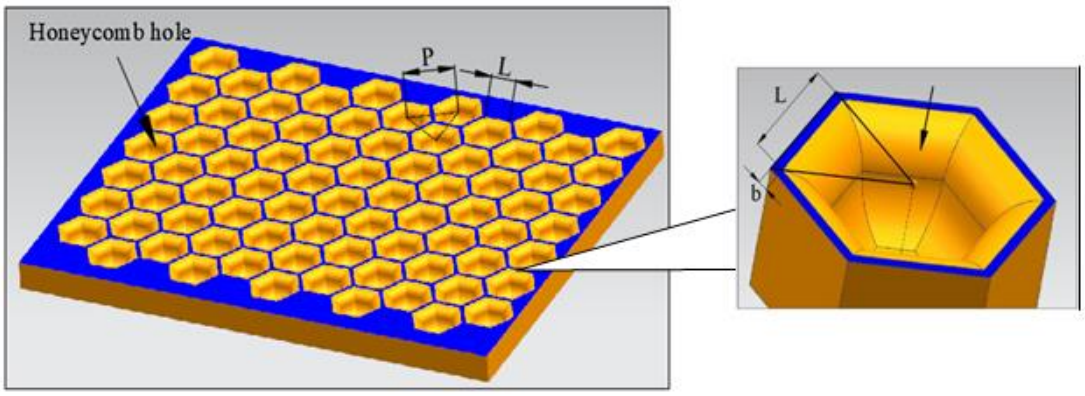

Fig.1 Model of the designed honeycomb structure

The cross-sectional profile of the side wall of a honeycomb hole conforms to the distribution of a Gaussian curve (Fig.2. (b)), that is, the shape of the sidewall and the depth of the structure should conform to those attainable by laser processing. Theoretically, the 2D profile of the micro-holes can be described by a Gaussian function as shown in Eq. (1).

$$z = -a \times e^{-\frac{x^2}{2c^2}} \tag{1}$$

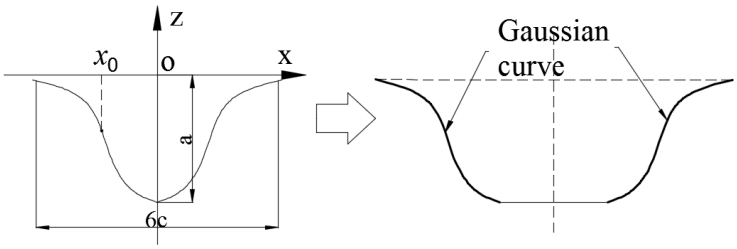

(a) (b)

Fig.2 Gaussian intensity profile of the laser beam and cross-section of honeycomb structure

Where *a* is Gaussian constant, and *c* is the standard deviation. In the Gaussian curve shown in Fig.2(a), the area proportion between -3*c* and +3*c* is about 99.7%, so the curve between ±3*c* is chosen to represent the Gaussian hole machined by the pulsed laser. The parameter *a* is the depth of the Gaussian hole and the parameter 6*c* is the width of the hole.

4. Experimental setup details

4.1 Experimental setup and operational procedure

Experimental setup: The laser machining experiments were carried out on a hybrid ultra-precision machine (Micro-3D) shown in Fig. 3. The machine was developed by the centre for Precision Manufacturing, DMEM of the University of Strathclyde and Ultra Precision Motion Ltd. It employs

aerostatic bearing guideways, Renishaw linear encoders and an A3200 Aerotech controller to achieve a motional accuracy of better than 0.2 μm for all four linear(X, Y, Z and W) axes. The machine is equipped with a nanosecond pulsed fibre laser which has a central emission wavelength of 1064 nm. The laser source has a nominal average output power of 20 W and its maximum pulse repetition rate is 200 kHz. During operation, the laser beam passes through a lens and focuses on the specimen surface which is mounted on a precision X-Y-C stage.

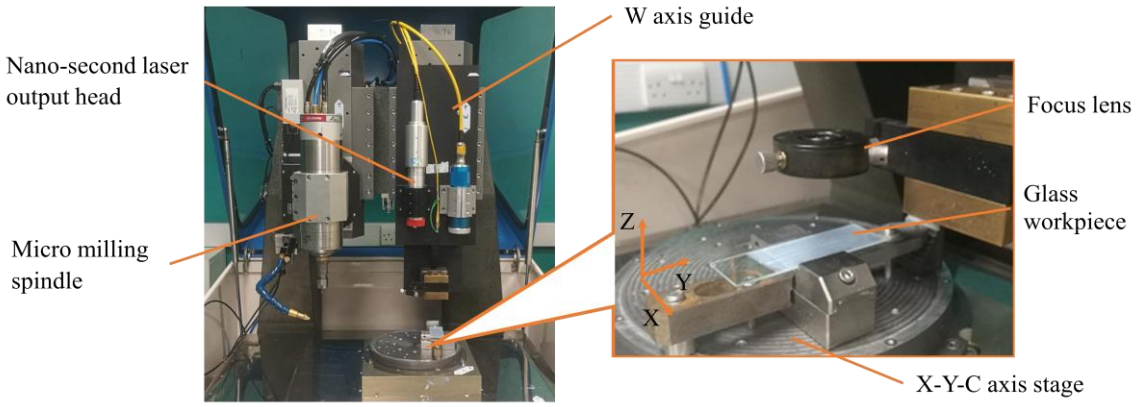

Fig.3 Illustration of experimental setup

Operational procedure: A precision micro-motion vice mounted on the X-Y-C work table is used to position and clamp the glass substrate. The fixture has a positioning accuracy of 1μm and a flatness number of 100 to ensure that the side of the glass coated with TiO_2 faces directly upwards. The focus position of the laser can be adjusted by taking the upper surface of the glass substrate as the reference zero point. After the start of laser processing, in order to target light-absorbing auxiliary materials, the focus position of the laser was offset upward by a certain distance to ensure that the laser was focused inside the auxiliary material layer(as shown in Fig4(b)). At the same time, the motion of the XY stage was used to feed the glass substrate. The laser cutting path during processing is shown in Fig.4 (a). The tool will start from the centre of the honeycomb hole and feeds in the order of "0→1→2→3… →1→7→8…". Each hole is processed in turn.

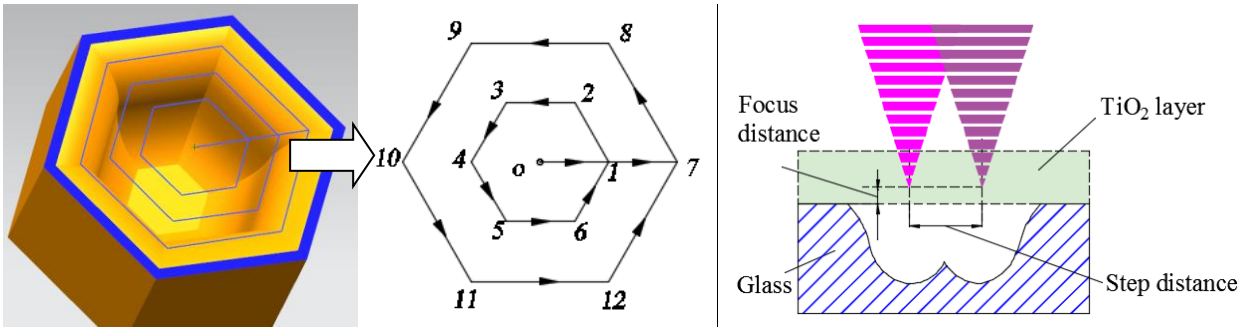

(a) (b)

Fig.4 Cutting path of Laser machining

4.2 Experimental planning and parameters selection

Parameters selection: The accuracy of the shape and size of the honeycomb depends on the shape of the Gaussian curved surface formed by the last path of the tool. The shape parameters of the Gaussian surface are controlled by Gaussian constant *a* and standard deviation *c*, while indirectly related to the basic parameters of the laser. Therefore, the basic parameters of the laser, (power and frequency) are selected as the main laser control parameters that affect the honeycomb structure.

The bottom of the honeycomb structure is produced by laser cutting, following all the paths (including the last path). The tool path will affect the surface quality and roughness of the honeycomb structure. Therefore, the feed rate of the laser beam and the distance between adjacent tool paths (Fig.4 (b)) will have major impacts on surface roughness, which is related to the transparency of the glass. Adjustment of the laser focal distance will affect the width of the laser beam scanning through the workpiece, which is related to the distance of the tool path, i.e. step distance. Therefore, the feed rate and laser focal distance are the principal processing parameters that affect light transmission.

Experimental planning: In pre-experiment micro-grooving trials, it was found that the laser power should be maintained below 30% of the rated power (that is, 6W) to ensure that no cracks appear on the glass surface. The measured *a* and 6*c* are 2.1μm and 18.2μm, respectively, under a laser power of 10% (that is, 2W) and a frequency of 15kHz. In this paper, the experimental research was carried out using 4-factor, 4-level (i.e. $L_{16}(4^4)$) according to the orthogonal experiment design method. The laser machining parameters are listed in Table 1. According to the data in Table 1, it takes about

25~40 minutes to process a sample with an area of 5mm by 5mm as laser scanning occurs through motion of the worktable in this experiment. For industrial application, a laser scanning head can be used to improve the processing efficiency. It will only take 6 seconds for processing microstructures in an area of 5mm by 5mm.

Table 1 The laser parameters in the experiments.

Laser power (W)	Pulse frequency (KHz)	Feed rate (mm/min)	Focus distance(mm)
2, 3, 4, 5	40,55,70,85	10,30,50,70	0,0.1,0.2,0.3

4.3 Pre- and post-processing of glass specimens and surface characterisation

Pre-processing: The glass microscope slide (Type CAT. No.7101.) is washed in clean water and then bathed in an ultrasonic cleaning machine for 5 minutes. After drying, the titanium dioxide solution is evenly spread on the surface of the glass slide, placed in cool and dry room, and left to stand horizontally for 48 hours.

Before laser processing, the surface of the glass needs to be coated with a light-absorbing auxiliary material, in which the auxiliary material used TiO_2 and was prepared into an aqueous solution with a solid content of 10%. The glass slide should firstly be installed horizontally on a fixture, which is connected to a two-dimensional precision workbench to achieve two-dimensional movement in the horizontal plane. During coating, the auxiliary material is dropped on the surface of the glass sheet, and the working table is controlled to move in the horizontal direction to ensure that the auxiliary material solution uniformly covers the glass sheet under a certain pressure. The coated TiO_2 layer improves the absorption of laser energy into glass specimens.

Post-processing: After laser machining, the specimens are rinsed with deionised water in ultrasonic cleaning equipment for half an hour to remove the molten slag and titanium dioxide on the surface. Then, these specimens are degreased in a 30-min ultrasonic bath in acetone followed by ethanol. Finally, these specimens are dried in an oven. Before measuring the contact angle, these specimens are silanized in a vacuum oven using silane reagent (1H, 1H, 2H, 2H Perfluorooctyltriethoxysilane, 97%, Alfa Aesar Ltd), at 100°C for 12 hours to reduce their surface free energies.

Surface measurement: The 2D profiles of machined microgrooves were measured by a Mitutoyo surface roughness measuring system (Surftest SV-2000/3000). The morphology of the lasered grooves was measured by a Dino-lite Digital Microscope (AM4115TW). The morphology of the lasered structure was measured by a Zygo white light interferometer (CP300). The light transmission performance of the workpiece in a natural state was tested by placing the glass substrate on a cardboard with some texts (See the text "Laser" in Figure 10 (1-4).) and observing the clearness of the text through the processed area and the non-processed area. Apparent contact angle on surfaces was measured by an industrial camera (UltraMacro 5X). The selected water droplet volume was 5 μL. For each specimen, the apparent contact angle of the water droplet was measured three times and the average value was adopted.

5. Results and discussions

The influences of processing parameters set by the orthogonal test design method shown in Table 1 on the fabricated microstructures will be discussed in this section.

5.1 Influence of laser processing parameters on honeycomb structures

In order to obtain honeycomb micro structures close to the designed geometries, the influence of basic laser processing parameters, i.e. the power and frequency, on the shape and dimension of the fabricated microstructures were studied in this paper. Fig. 5 shows the photomicrographs of the fabricated microstructures under different laser powers.

It can be seen from Fig 5(a-d) that, with the increase of laser power, the honeycomb shape becomes irregular and the wall thickness of the honeycomb becomes thinner and thinner. In other words, the size of the honeycomb cavities increases with the laser power. At the same time, the measured depth of honeycomb (about 5.75~6.5μm) of each machined surface is unchanged, indicating that the cavity depth is unchanged. This is mainly because the increase of laser power will result in the decrease of the standard deviation c value of the Gaussian distribution. A larger value of c will produce wider Gaussian micro-hole, which will cause the honeycomb cavity to expand outward.

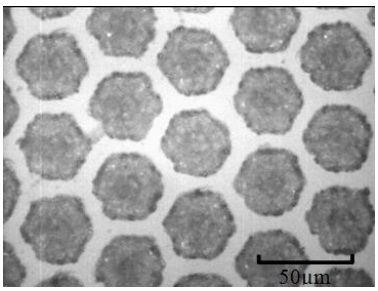

(a) Power 10%

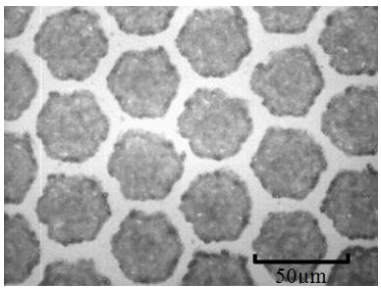

(b) Power 15%

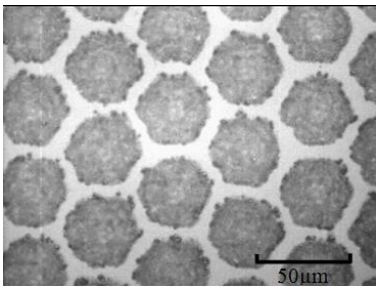

(c) Power 20%

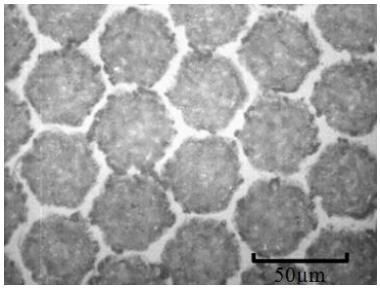

(d) Power 25%

Fig. 5 Microphotograph at different laser powers（Laser frequency is 40 kHz, Feed rate is 50mm/min and Focus distance is 0.2mm）

Fig. 6 shows that the wall thickness of the honeycomb structure remains the same while changing the laser pulse frequency, however, the shape of the honeycomb microstructures become irregular with the increase of laser pulse frequency. A close examination of Fig.6 (b) (c) and (d), it is found that the materials at the structural grooves have been melted. This is because with the increase of laser pulse frequency, leads to a short the interval time between each laser pulses, then the cooling time on the glass surface is reduced. The accumulation of more thermal energy will melt the glass and ultimately deform the overall honeycomb structure.

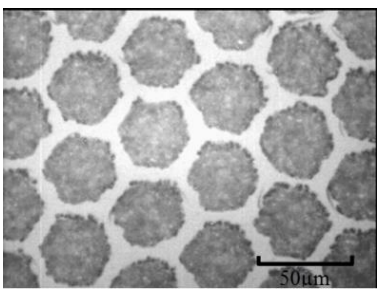

(a) 40 kHz

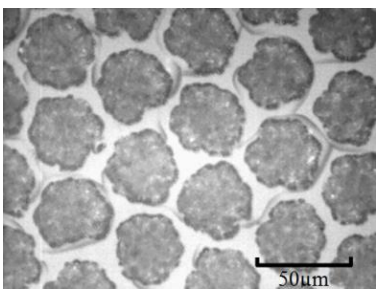

(b) 55 kHz

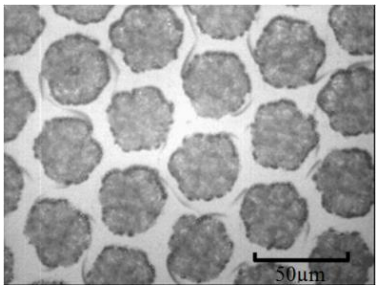

(c) 70 kHz

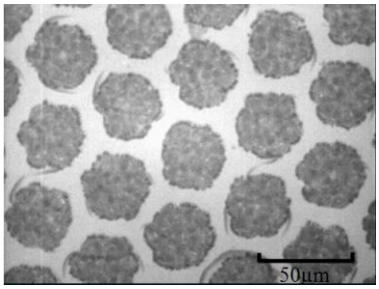

(d) 85kHz

Fig. 6 Microphotograph at different laser frequencies (Laser power is 25%, Feed rate is 50mm/min and Focus distance is 0.2mm)

5.2 Influence of laser processing parameters on light transmission

As glass is mostly used for optical application, it is vital to ensure its light transmittance after generation of anti-fogging microstructures as much as possible. The transparency of materials is mostly related to the machined surface roughness. Fig. 7 shows measured surface topography of specimens which were processed at different distance to the laser focal point.

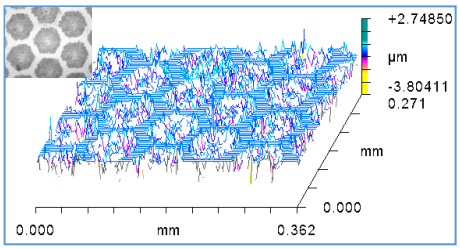

(a) Focus distance=0.3 mm

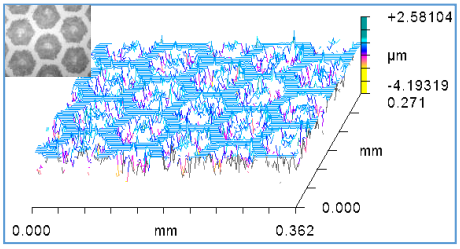

(b) Focus distance =0.2mm

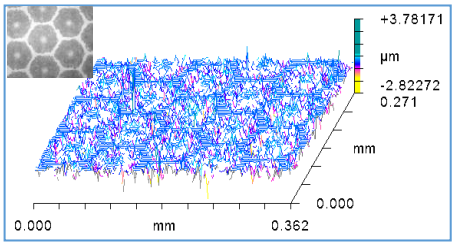

(c) Focus distance =0.1 mm

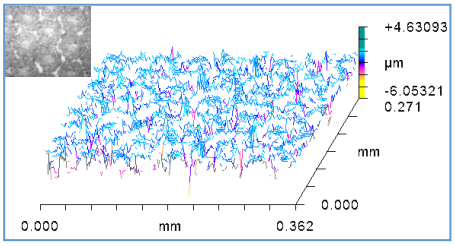

(d) Focus distance =0mm

Fig. 7 Microphotograph the machined surfaces processed at different laser focus distance (Laser power is 25%, Feed rate is 50mm/min and Laser frequency is 40 kHz)

When the focal point was far away for the top surface of glass specimen, as shown in Fig.7 (a) and (b), accurate microstructure shape was obtained. However, when the laser focal point got closer to the top surface, more materials were observed to be burned severely and to form irregular honeycomb structures, as shown in Fig.7(c) and (d). In the four cases from (a) to (d), the depth of

the measured micro grooves was 2.4μm, 2.5μm, 3.0μm, and 4.6μm, respectively. That is to say, the smaller the focal distance, and the larger the depth of the obtained microcavity structure.

The processed surfaces obtained at different feed rates are shown in Fig. 8. It can be seen that a regular honeycomb structure can be obtained. In all four cases, it is found that the depth of the microcavity measured is around 3.0μm. This indicates that the feed rate has little effect on the machined surface roughness under the testing range in this paper.

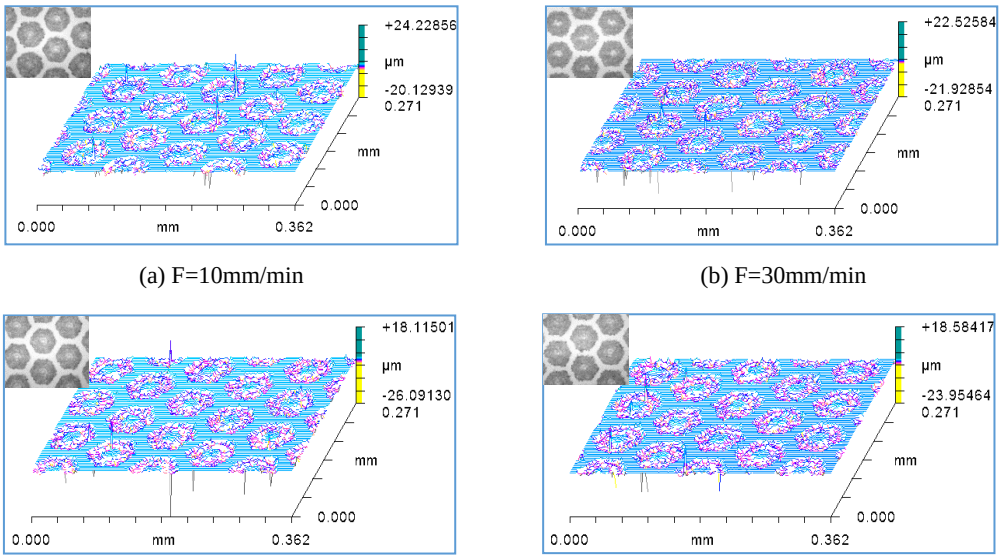

(a) F=10mm/min (b) F=30mm/min

(c) F=50mm/min (d) F=70mm/min

Fig.8 Microphotographs of the surfaces at different feed rates (Laser power is 25%, Laser frequency is 40 kHz and Focus distance is 0.2mm)

The reasons for the above phenomenon are as follows: when the focus position of the laser is close to the surface of the processed glass, that is, a downward displacement of Δd as shown in the Fig.9, the energy absorbed by the workpiece will increase (the area of the shaded area in the figure represents energy) and the position of the affected area of the laser beam also moves down accordingly, which inevitably leads to an increase in the depth of the processed cavities. At the same time, the downward movement of the focal position will causes the increase of the scanning width of the laser beam across the surface of the workpiece, and the volume of the repeatedly processed material (the overlapping area of the shadow in the right figure), so it will cause the glass material to burn more severely. Similarly, when the feed rate of the laser is changed without

changing the focus position, the energy absorbed by the glass workpiece is essentially unchanged, and the depth and surface quality of the micro cavity are also unchanged.

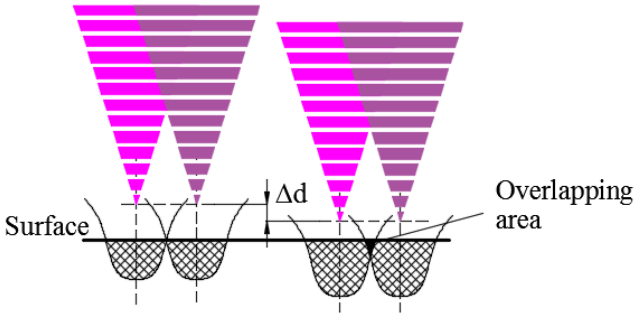

Fig.9 Laser processing diagram

The influence of focus distance and feed rate on the light transmittance was studied. To simplify the analysis we only selected results from four light transition tests which corresponded to the medium and highest focus distances and medium and high feed rates respectively.

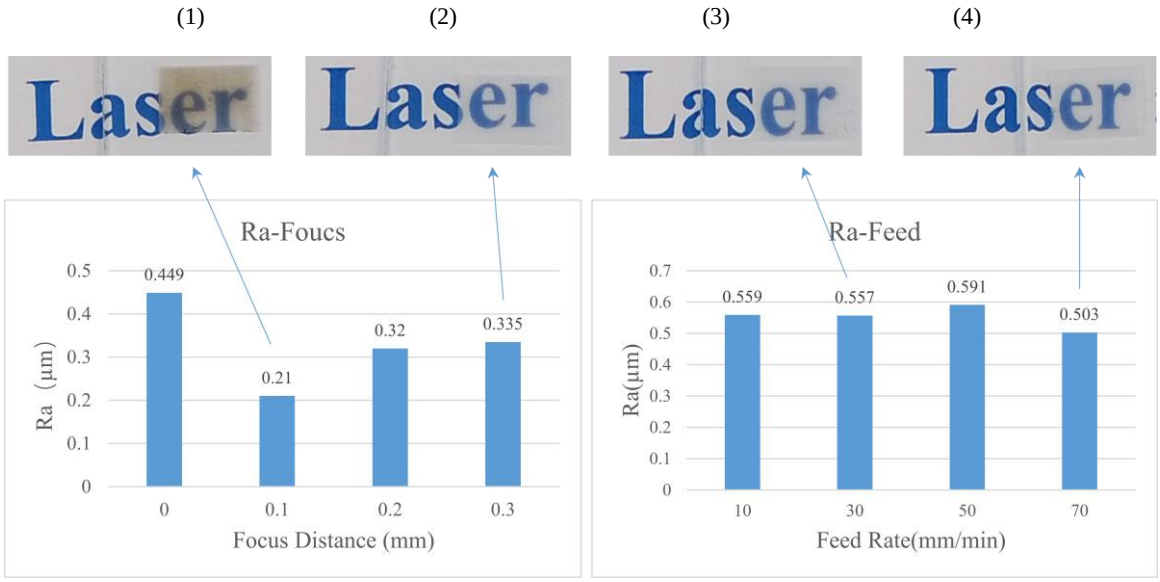

(a) (b)

Fig. 10 Surface roughness of the machined surfaces processed at different feed rate or focus distance

The upper part of Fig. 10 shows the result of light transitions of the glass sheet obtained in the above four cases. In the first case (Fig. 10(1)), because the focus is too close to the surface, the ablation damage phenomenon is severe, which affects its light transmission although its surface roughness is the smallest of the four cases. In the second case (shown in Fig.10(2)), there is no severe burn and better light transmission is achieved. This shows that the burn of the material

caused by the change of the focal distance is an important determinant of light transmittance. The three cases (shown in Fig.10(2),(3) & (4)) have better light transmittance than the case shown in Fig.10(1)as no material burns appeared. Among the cases light transmittance of the second case (shown in Fig.10 (2)) is slightly better than that of Fig.10 (3) and (4). According to Ying et al's study[44], this is because a better roughness value results in less light being reflected back and refracted when the light passes through the surface, which means, more transmitted light. Therefore, almost the same surface roughness value for case 3 (Fig.10 (3)) and case 4(Fig.10 (4)) results in a very similar level of transmission ability. However, light transmittance by the proposed laser processing approach is bound to be an important and challenging issue, especially when compared with coating technology. Further improvement of light transmittance is required in future research.

5.3 Analysis of surface hydrophilicity and contact angle.

In this study, static contact angles of water droplets were measured using the sessile drop method to characterize the wettability of the specimen surfaces, including a smooth glass surface as a benchmark. The sessile drop method is a way to directly assess wetting properties of a solid surface and to measure the contact angle of water droplets placed on the surface [45][46]. The contact angle was measured based on the side view of a water drop, which was captured using an industrial macro lens camera.

Fig.11 shows the measured surface topography of white light interference photograph with corresponding measured surface contact angle. The measurement results show that the honeycomb resulted in a reduced surface contact angle. The contact angle decreases with the decrease of the structure pitch. At a side length of 10 microns, the contact angle reached 4.7 ° (<5 °), indicating that a super-hydrophilic surface has been obtained.

The reason for this phenomenon is that when the structure size of the micropores is large, the gas in the honeycomb holes provides sufficient surface energy, which inhibits the movement of water droplet to the bottom of the holes, resulting in poor hydrophilicity of the surface. Conversely, a

decrease in structure size leads to a decrease in surface energy of water droplet, which makes it easier to produce hydrophilic and super-hydrophilic results.

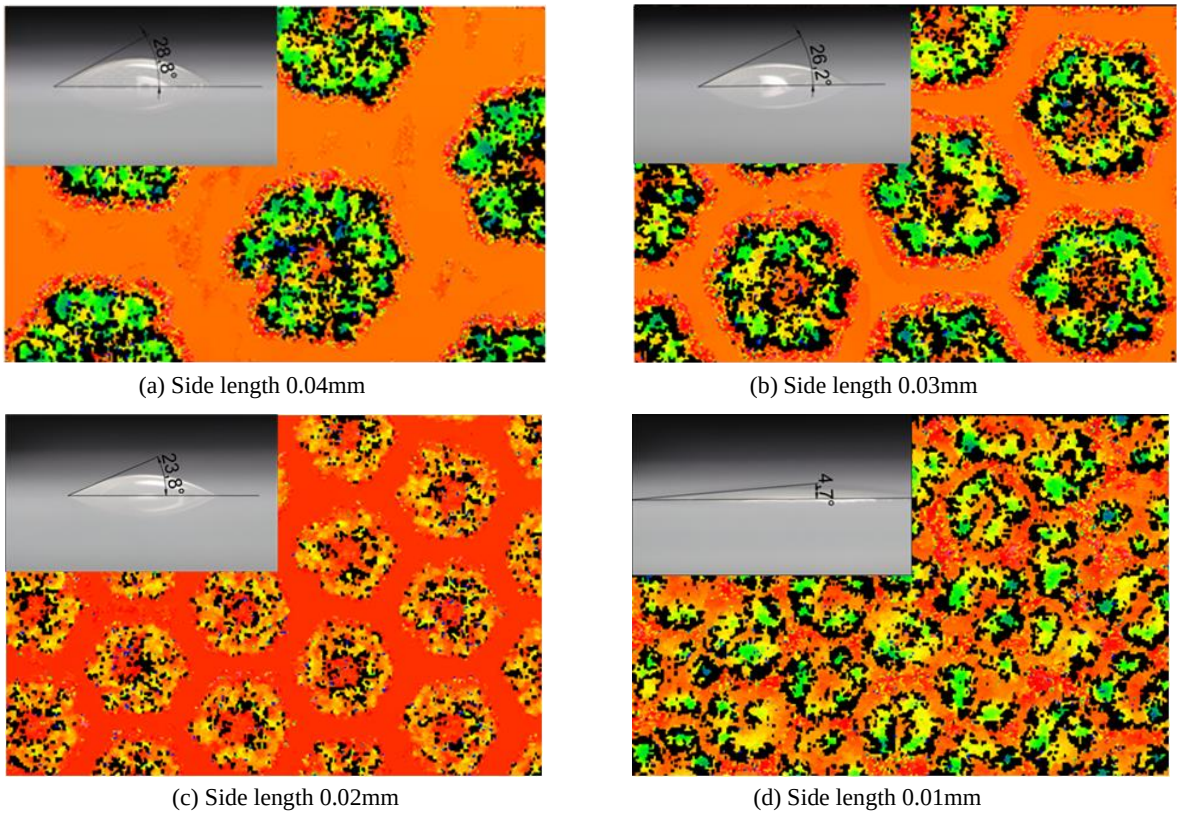

(a) Side length 0.04mm (b) Side length 0.03mm

(c) Side length 0.02mm (d) Side length 0.01mm

Fig.11 Measured surface topography and contact angle at different side size

6. Conclusions

In this paper, a nanosecond laser ablation method for glass surface assisted by light-absorbing material was proposed, and anti-fogging, microstructures were successfully formed on glass. The effects of laser power, frequency, surface roughness *Ra* and structure size on the hydrophilicity of the glass surface were investigated through nanosecond laser processing experiments on the surface of glass sheets. The following conclusions can be drawn:

1. Assisted by light-absorbing auxiliary materials nanosecond laser processing can be used to successfully obtain super-hydrophilic microstructures without compromising the transparency of glass.
2. Lower laser power (about 3W) and lower frequency (less than 40 kHz) are the key to realize regular honeycomb structures on glass by using nanosecond laser processing.

3. The distance from the top glass surface to the laser focal point will greatly affect the light transmittance of the processed glass, and a distance of 0.1-0.2mm is the recommended range in this article. The feed rate is found to have little influence on light transmission under the testing range used here.
4. Surface contact angle decreases as the pitch of the honeycomb structure decreases. Super-hydrophilic glass surface can be achieved when the length of the honeycomb structure is about 10 microns.

Declaration of competing interests

The authors declared that they have no conflicts of interest in this work.

Acknowledges

This work was supported by the EPSRC_(EP/K018345/1, EP/T024844/1), Royal society-NSFC International exchange scheme(IEC/NSFC/181474). The authors would also gratefully acknowledge the financial support from the China Scholarship Council (CSC).

Data statement

All data underpinning this publication are openly available from the University of Strathclyde's Knowledge Base.

References

[1] Ohdaira T, Nagai H, Kayano S, Kazuhito H. Antifogging effects of a socket-type device with the superhydrophilic, titanium dioxide–coated glass for the laparoscope. Surg Endosc 2007; 21(2):333–8. https://doi.org/10.1007/s00464-006-0795-8.

[2] Hashimoto D, Shouji M. Development of a fogless scope and its analysis using infrared radiation pyrometer. Surg Endosc 1997; 11(4):805–8. https://doi.org/10.1007/s004649900458.

[3] Liu XM, He JH. Progress in antifogging technology—from surface engineering to functional surfaces. Prog chem 2010; 22:270-276. https://doi.org/ 10.1631/jzus.B1000073

[4] Kwadwo E. Tettey, Majemite I. Dafinone, Daeyeon Lee. Progress in Superhydrophilic surface development. Mater Express 2011;1(2):89-104. https://doi.org/10.1166/mex.2011.1021.

[5] Dong HC, Ye PL, Zhong MJ, Pietrasik J, Drumright R, Matyjaszewski Krazysztof. Superhydrophilic Surfaces via Polymer−SiO2 Nanocomposites. Langmuir. 2010; 26(19):15567-15573. https://doi.org/10.1021/la102145s.

[6] Kapil M, Shantanu B. Superhydrophobic surfaces review: Functional application, fabrication techniques and limitations. J Micromanuf 2019; 2(1):59–78. https://doi.org/10.1177/ 2516598419836345.

[7] Gao YF, Masuda Y, Koumoto K. Light-Excited Super hydrophilicity of Amorphous TiO2 Thin Films Deposited in an Aqueous Peroxotitanate Solution. Langmuir 2004; 20(8):3188-3194. https://doi.org/10.1021/la0303207.

[8] Norrman K, Ghanbari-Siahkali A, Larsen N. B.. Studies of spin-coated polymer films. Annu Rep Prog Chem Sect C Phys Chem 2005; 101(4):174-201. https://doi.org/10.1039/ B408857N.

[9] Zheng BX, Wang WJ, Jiang GD, Wang KD, Mei XS. Research status and application prospects of manufacturing technology for micro–nano surface structures with low reflectivity. Proc Inst Mech Eng Part B: J Eng Manuf 2014;229(11):1877–1892. https://doi.org/10.1177/ 0954405414542113.

[10] Varahramyan K, Lvov Y. Nanomanufacturing by layer-by-layer assembly – from nanoscale coating to device applications. Proc Inst Mech Eng Part N: J. Nanoeng Nanosyst. 2006; 220(3):29-37. https://doi.org/10.1243/17403499JNN47.

[11] Huang WX, Lei M, Huang H, Chen JC, Chen HQ. Effect of polyethylene glycol on hydrophilic TiO2 films: Porosity-driven superhydrophilicity. Surf Coat Technol. 2010; 204(3):3954-3961. https://doi.org/10.1016/j.surfcoat.2010.03.030.

[12] Wang DA, Guo ZG, Chen YM, Hao JC, Liu WM. In Situ Hydrothermal Synthesis of Nanolamellate CaTiO3 with Controllable Structures and Wettability. Inorg Chem. 2007; 46(4):7707-7709. https://doi.org/10.1021/ic700777f .

[13] Pathan H M, Lokhande C D. Deposition of metal chalcogenide thin films by successive ionic layer adsorption and reaction (SILAR) method. Bull Mater Sci 2004; 27(2):85-111. https://doi.org/10.1007/BF02708491.

[14] Hosono E, Matsuda H, Honma I, Ichihara M, Zhou HS. Synthesis of a Perpendicular TiO2 Nanosheet Film with the Superhydrophilic Property without UV Irradiation. Langmuir 2007; 23(5):7447-7450. https://doi.org/10.1016/j.mssp.2020.104927 .

[15] Hao XQ, Li J, Song XL, Wang L, Li L. Roughness effect for tunable wetting surfaces on metallic substrate. Proc Inst Mech Eng Part B: J Eng Manuf 2018; 232(5): 787–796. https://doi.dox.org/10.1177/0954405416654191.

[16] Azarsa E, Ibrahim A, Papini M. Abrasive water and slurry jet micro-machining techniques for fabrication of molds containing raised free-standing micro-features. Precis Eng. 2020;65:197-215. https://doi.org/10.1016/j.precisioneng.2020.05.009.

[17] Azarsa E, Cinco L, Papini M. Fabrication of high aspect ratio free-standing structures using abrasive water jet micro-machining. J Mater Proc Tech. 2020; 275:116318. https://doi.org/10.1016/j.jmatprotec.2019.116318.

[18] Zhou Y, Wu BX. Experimental study on infrared nanosecond laser-induced backside ablation of sapphire. J Manuf Proc 2010;12:57-61. https://doi.org/10.1016/j.jmapro.2010.02.002.

[19] Zhang HZ, Huang T, Liu Z, Zhang X, Lu JL, Xiao RS. High fluence nanosecond laser machining of SiCp/AA2024 composite with high pressure assistant gas. J Manuf Process 2018;31:560-567. https://doi.org/10.1016/j.jmapro.2017.12.020.

[20] Cheong HG, Chu CN, Kwon KK, Song KY. Micro-structuring silicon compound ceramics using nanosecond pulsed laser assisted by hydrothermal reaction. J Manuf Process 2020;50:34-46. https://doi.org/10.1016/j.jmapro.2019.12.005.

[21] Teixidor D, Thepsonthi T, Ciurana J, Özel T. Nanosecond pulsed laser micromachining of PMMA-based microfluidic channels. J Manuf Processes 2012;14:435-442. https://doi.org/10.1016/j.jmapro.2012.09.001.

[22] Kam DH, Kim J, Mazumder J. Near-IR nanosecond laser direct writing of multi-depth microchannel branching networks on silicon. J Manuf Processes 2018;35:99-106. https://doi.org/10.1016/j.jmapro.2018.07.023.

[23] Razi S, Mollabashi M, Madanipour K. Nanosecond Laser Surface Patterning of Bio Grade 316L Stainless Steel for Controlling its Wettability Characteristics. Int J Opt Photo. 2015; 9(1):43-52. http://ijop.ir/article-1-184-en.html

[24] Rafieazad M, Jaffer JA, Cui C, Duan XL, Nasiri A. Nanosecond Laser Fabrication of Hydrophobic Stainless Steel Surfaces: The Impact on Microstructure and Corrosion Resistance. Mater 2018;11:1577. https://doi.org/10.3390/ma11091577.

[25] Cai YK, Chang WL, Luo XC, Sousa AML, Lau KHA, Qin Y. Superhydrophobic structures on 316L stainless steel surfaces machined by nanosecond pulsed laser. Precis Eng 2018;52:266-275. https://doi.org/10.1016/j.precisioneng.2018.01.004.

[26] Emelyanenko AM, Shagieva FM, Domantovsky AG, Boinovich LB. Nanosecond laser micro- and nanotexturing for the design of asuperhydrophobic coating robust against long-term contact withwater, cavitation, and abrasion. Appl Surf Sci 2015;332:513-517. https://doi.org/10.1016/j.apsusc.2015.01.202.

[27] Phys. Zaimis U, Biol. Aleksejeva JV, Aleksejevs R, Math. Guseynov Sh.E. Hydrophilic nanostructure formation on the titanium surface by direct laser irradiation. Mach Tech Mater. 2017; 8(11):407-412. https://stumejournals.com/journals/mtm/2017/8/407

[28] Klinger D, Łusakowska E, Z˙ymierska D. Nano-structure formed by nanosecond laser annealing on amorphous Si surface. Mater Sci Semicond Process 2006;9:323-326. https://doi.org/10.1016/j.mssp.2006.01.027.

[29] Krishna H, Favazza C, Gangopadhyay AK, Kalyanaraman R. Functional nano- structures through nanosecond laser dewetting of thin metal films. Mater Coat 2008;9(60):36-42. https://doi.org/10.1007/s11837-008-0115-y.

[30] Lavieja C, Oriol L, Peña JI. Creation of Superhydrophobic and Superhydrophilic Surfaces on ABS Employing a Nanosecond Laser. Mater 2018; 11:2547. https://doi.org/10.3390/ ma11122547.

[31] Lawrence J, Li L. Wettability characteristics of polyethylene modified with CO2,Nd:YAG, excimer and high-power diode lasers. Proc Inst Mech Eng Part B J Eng Manuf. 2001; 215(4):1735-1744 . https://doi.org/10.1177/095440540121501207.

[32] Zhao JN, Guo J, Shrotriya P, Wang Y, Han YF, Dong YH, Yang S. A rapid one-step nanosecond laser process for fabrication of superhydrophilic aluminum surface. Opt Laser Tech 2019; 117(4):134-141. https://doi.org/10.1016/j.optlastec.2019.04.015.

[33] Samanta A, Wang QH, Singh G, Shaw SK, Toor F, Ratner A, Ding HT. Nanosecond pulsed laser processing turns engineering metal alloys antireflctive and superwicking. J Manuf Process 2020; 54: 28-37. https://doi.org/10.1016/ j.jmapro.2020.02.029

[34] Zhou M, Huang T, Cai L. The novel nanosecond laser micro-manufacturing of three-dimensional metallic structures. Appl Phys A 2008;90:293-297. https://doi.org/10.1007/s00339-007-4269-1

[35] Jagdheesh R, Garcia-Ballesteros JJ, Ocana JL. One-step fabrication of near super hydrophobic aluminum surface by nanosecond laser ablation. Appl Surf Sci 2016;374:2-11. https://doi.org/10.1016/j.apsusc.2015.06.104.

[36] Zhu HZ, Zhang HC, Ni XW, Shen ZH, Lu J. Fabrication of superhydrophilic surface on metallic nickel by sub-nanosecond laser induced ablation. AIP Adv 2019:085308. https://doi.org/10.1063/1.5111069@adv.2019.PO2019.issue-1

[37] Chun DM, Ngo CV, Lee KM. Fast fabrication of superhydrophobic metallic surface using nanosecond laser texturing and low-temperature annealing. CIRP Ann Manuf Technol. 2016;65:519-522. https://doi.org/10.1016/j.cirp.2016.04.019.

[38] Guan YC, Zhou W, Zheng HY,Li ZL. Solidification microstructure of AZ91D Mg alloy after laser surface melting. Appl Phys A 2010;101:339-344. https://doi.org/10.1007/s00339-010-5880-0

[39] Yang Z, Tian YL, Yang CJ, Wang FJ, Liu XP. Modification of wetting property of Inconel 718 surface by nanosecond laser texturing. Appl Surf Sci. 2017;414:313-324. https://doi.org/ 10.1016/j.apsusc.2017.04.050.

[40] Nikumb S, Chen Q, Li C, Reshef H, Zheng HY, Qiu H, Low D. Precision glass machining, drilling and profile cutting by short pulse lasers. Thin Solid Films 2005; 477 (10) :216– 221. https://doi.org/10.1016/j.tsf.2004.08.136.

[41] Pan YX, Lv XM, Zhang HC, Chen J, Han B, Shen ZH, Lu J, Ni XW. Millisecond laser machining of transparent materials assisted by nanosecond laser with different delays. Opt lett 2016; 41(12):2807-2810. https://doi.org/10.1364/ OL.41.002807

[42] Abbott SJ, Gaskell PH. Mass production of bio-inspired structured sur faces. Proc. Inst Mech Eng Part C: J. Mech Eng Sci 2007;221:1181-1191. https://doi.org/10.1243/09544062 JMES540

[43] Liu KS, Yao X, Jiang L. Recent developments in bio-inspired special wettability. Chem Soc Rev 2010; 39(6):3240–325 . https://doi.org/10.1039/B917112F

[44] Ying JX, Zhang B, Cui X, Xu XZ. Influencing factors of transmittance of laser transparent ceramics. High power laser part beams. 2011;23(3):581-585. https://doi.org/10.3788/HPLPB 20112303.0581.

[45] Staicopolus DN. The computation of surface tension and of contact angle by the sessile-drop method. J colloid sci 1962(17):439-447. https://doi.org/10.1016/0095-8522(62)90055-7.

[46] Bachmann J, Horton R, Van der Ploeg RR, Woche S. Modified sessile drop method for assessing initial soil-water contact angle of sandy soil. Soil Sci Soc of Am J. 2000;64(3):564-567 . https://doi.org/10.2136/sssaj2000.642564x